JOURNAL OF MATERIALS SCIENCE 33 (1998) 3519–3524

Influence of crystallization conditions on the structural characteristics of poly(*p*-phenylene sulfide): Rietveld refinement

P. BALLIRANO
Corso Duca di Genova 147, I-00121, Rome, Italy

R. CAMINITI
Dipartimento di Chimica, Istituto Nazionale per la Fisica della Materia, Università di Roma "La Sapienza", P. le A. Moro 5, I-00185, Rome, Italy

L. D'ILARIO, A. MARTINELLI, A. PIOZZI
Dipartimento di Chimica, Università di Roma "La Sapienza", P. le A. Moro 5, I-00185, Rome, Italy
E-mail: dilario@axcasp.caspur.it

A. MARAS
Dipartimento di Scienze della Terra, Università di Roma "La Sapienza", P. le A. Moro 5, I-00185, Rome, Italy

A study was undertaken to obtain more accurate structural information on poly(*p*-phenylene sulfide) (PPS) through Rietveld analysis. A few samples of PPS crystallized in a relatively wide range of physical conditions were selected with the aim of eventually identifying the occurrence of structural modifications induced by the various crystallization procedures. According to the results, the structural modifications are relatively small and essentially confined to variations of the C–S–C angle, for which values within the range 102°–105° were found close to those proposed by Garbarczyk. In particular, the strong influence of the amorphous phase in determining the crystallographic cell dimension was investigated.

1. Introduction

Poly (*p*-phenylene sulfide) (PPS) is an engineering thermoplastic material [1] that has received much attention in the last decade for its outstanding physical (mechanical, thermal, electrical) and chemical (stability) properties in both the academic and industrial fields. Its semicrystalline nature, on the other hand, make it suitable for accurate studies of its structural and physical properties in either the crystalline [2–9] or the amorphous state [10, 11]. These researchers have obtained different results for the crystal structure of this polymer although the initial Tabor [2] model seems to be fundamentally correct. Its determination was carried out from fibre photographs using 2θ independent reflections, whose intensities were visually estimated. The semi-quantitative structure analysis indicated four monomeric units in the orthorhombic unit cell (space group P*bcn*-D_{2h}, $a = 0.867$ nm, $b = 0.561$ nm, $c = 1.026$ nm). The repeating units are distributed within two chains, one passing through the centre, the other through a corner of the unit cell. The sulphur atoms are arranged in a zig-zag trans-planar conformation, lying in the (1 0 0) plane, whereas the phenyl rings are alternately rotated by $\pm 45°$ with respect to the (1 0 0) plane, forming a C–S–C angle of 110° (Fig. 1).

Subsequently, Garbarcyzk [3, 4], on the basis of PPS analogue structural studies, proposed a C–S–C angle of 103°–107°, resulting in a smaller unit cell parameter, *c*, of the order of 0.980–1.007 nm. Uemura *et al.* [5], from high-resolution electron microscopy experiments, confirmed the structure proposed by Tabor, and the same conclusion was drawn also by Lovinger *et al.* [6]. Chung *et al.* [7, 8] indicated, from powder diffraction X-ray data, that samples cold-crystallized at various temperatures and annealed for different times show substantial differences in lattice parameters. In fact, the PPS cell parameters found in the literature show significant scattering. In particular, *a* ranges from 0.854–0.873 nm, *b* from 0.557–0.566 nm and *c* from 0.980–1.037 nm.

In order to obtain more accurate structural information, a Rietveld refinement was carried out on powder diffraction X-ray data obtained from PPS samples originated under different physical conditions. The results of this investigation are discussed below.

2. Experimental procedure

PPS Ryton V-I powder ($\langle M_w \rangle = 14\,000$; Phillips Petroleum) was previously purified from low molecular

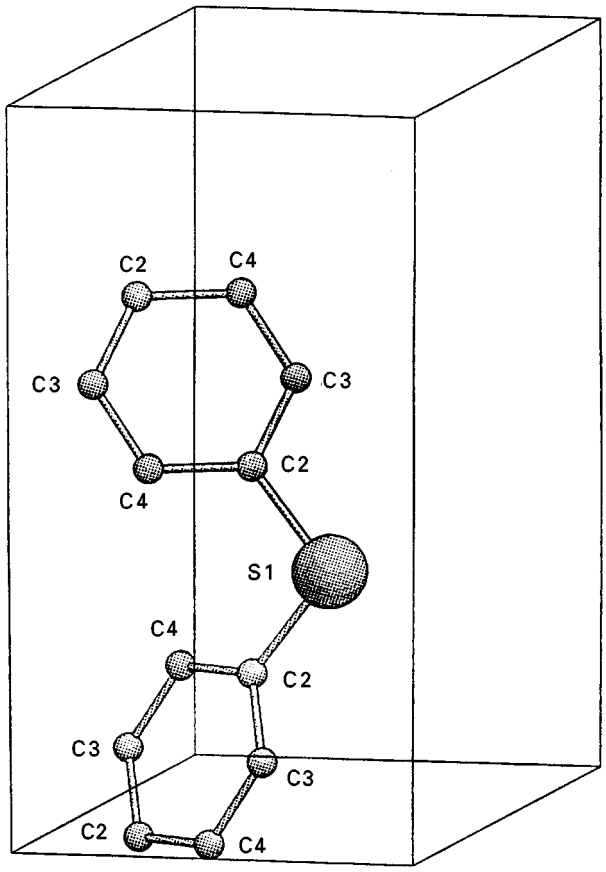

Figure 1 Conformation of PPS chain. Atoms are labelled according to the present Rietveld structure refinement. The unit cell is also indicated.

weight components by treatment in a Soxhlet column with tetrahydrofuran in order to remove all the low molecular weight species. Five different kind of PPS samples were then employed for the X-ray diffraction experiments:

1. powders of the as extracted PPS (e-PPS);
2. powders of single crystals obtained by crystallizing e-PPS from diphenyl ether solutions ($c = 0.25\%$) at $T_c = 190\,^{\circ}C$ for 48 h (c-PPS);
3. samples prepared by melting e-PPS powders on a glass surface within a brass ring, rapidly quenched in liquid nitrogen in order to maximize the amorphous fraction (a-PPS);
4. samples of a-PPS annealed at $T_c = 130\,^{\circ}C$ for 3 h in order to allow the polymer to crystallize from the solid amorphous state (ac130-PPS);
5. samples of a-PPS annealed at $T_a = 210\,^{\circ}C$ for 24 h (ac210-PPS).

The powders were loaded inside a 0.5 mm cavity of a conventional glass sample holder in order to minimize preferred orientation effects, while samples 3–5 were exposed to the X-ray beam on their smooth side, obtained on the glass-contact side, after removal of the glass. Data were collected on an automated Seifert MZ IV powder diffractometer, operating in the conventional $\theta/2\theta$ Bragg–Brentano geometry. The experimental details are given in Table I. The data were evaluated with the PC version of the well-known GSAS software package [12].

The starting atomic positional parameters used in the present Rietveld refinement were those of Tabor *et al.* [2]. Soft constraints on bond distances and angles were imposed, initially with high statistical weight, which was subsequently reduced during the refinement. The peak shape was modelled using a

TABLE I Experimental details of X-ray diffraction data collection

Diffractometer	Seifert MZ IV operating @40 KV and 30 mA
Radiation	CuK_α ($\lambda = 0.15406$ nm)
Soller slits	2: on incident and diffracted beams
Monochromator	Diffracted-beam pyrolitic graphite
2θ angular range	88–70°
Step	0.02°
Counting time	8 s

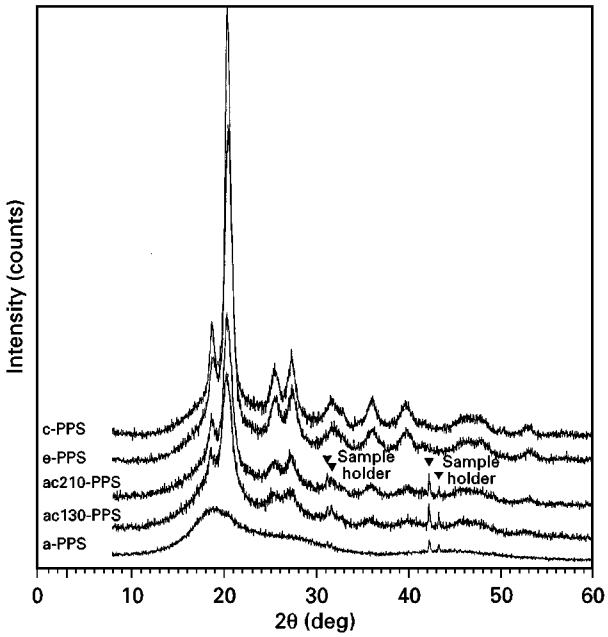

Figure 2 Experimental raw diffraction patterns.

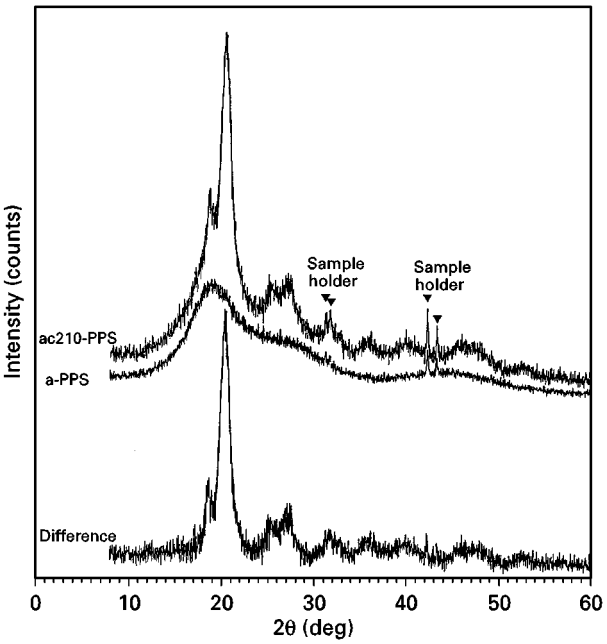

Figure 3 Example of the effect of the amorphous component subtraction.

TABLE II Miscellaneous data of the Rietveld refinements

	e-PPS	c-PPS	ac130-PPS	ac210-PPS
R_p	9.5%	9.9%	16.0%	14.9%
wR_p	13.6%	14.0%	22.2%	20.8%
R_{exp}	7.8%	7.8%	10.2%	10.4%
R_{Bragg}	5.3%	6.0%	16.2%	14.9%

TABLE III Fractional atomic coordinates and displacement parameters; (a) e-PPS; (b) c-PPS; (c) ac130-PPS; (d) ac210-PPS; (e) Tabor *et al.* [2]

		x	*y*	*z*	*B*
S1	a	0	0.333(1)	1/4	4.5(5)
	b	0	0.336(1)	1/4	4.4(3)
	c	0	0.322(2)	1/4	0.3(5)
	d	0	0.324(1)	1/4	2.5(5)
	e	0	0.322	1/4	
C2	a	− 0.002(2)	0.136(2)	0.387(1)	1.5(5)
	b	0.000(2)	0.142(2)	0.388(1)	1.5(5)
	c	− 0.018(3)	0.123(3)	0.383(1)	0.1(7)
	d	− 0.012(2)	0.128(3)	0.385(1)	1.6(6)
	e	0	0.143	0.389	
C3	a	− 0.096(1)	0.202(2)	0.493(1)	1.5(5)
	b	− 0.091(1)	0.208(2)	0.495(1)	1.5(5)
	c	− 0.088(2)	0.207(3)	0.497(1)	0.1(7)
	d	− 0.091(2)	0.205(2)	0.495(1)	1.6(6)
	e	− 0.099	0.196	0.492	
C4	a	− 0.085(2)	0.078(3)	0.608(1)	1.5(5)
	b	− 0.085(2)	0.074(2)	0.608(1)	1.5(5)
	c	− 0.091(2)	0.060(3)	0.607(1)	0.1(7)
	d	− 0.091(3)	0.062(3)	0.607(1)	1.6(6)
	e	− 0.099	0.053	0.604	
H5	a	− 0.198(6)	0.312(1)	0.472(3)	1.5(5)
	b	− 0.191(6)	0.321(1)	0.478(3)	1.5(5)
	c	− 0.181(6)	0.339(8)	0.486(3)	0.1(7)
	d	− 0.185(6)	0.332(9)	0.483(3)	1.6(6)
	e	− 0.175	0.379	0.486	
H6	a	− 0.176(6)	0.105(9)	0.679(4)	1.5(5)
	b	− 0.126(9)	0.152(9)	0.697(2)	1.5(5)
	c	− 0.202(6)	0.034(1)	0.657(3)	0.1(7)
	d	− 0.197(6)	0.053(1)	0.665(7)	1.6(6)
	e	− 0.175	0.095	0.684	

TABLE IV Relevant bond angles and distances (a) e-PPS; (b) c-pps; (c) ac130-PPS; (d) ac210-PPS; (e) Tabor *et al.* [2]

	Sample	Bond angle (deg)
C2–S–C2	a	104(1)
	b	105(1)
	c	102(1)
	d	103(1)
	e	110
		Bond distance (nm)
S1–C2	a	0.1784(5)
	b	0.1786(5)
	c	0.1764(7)
	d	0.1767(6)
	e	0.174
C2–C3	a	0.141(1)
	b	0.141(1)
	c	0.140(1)
	d	0.139(1)
	e	0.139
C2–C4	a	0.141(1)
	b	0.141(1)
	c	0.140(1)
	d	0.139(1)
	e	0.140
C3–C4	a	0.138(1)
	b	0.139(1)
	c	0.140(1)
	d	0.140(1)
	e	0.140
C3–H5	a	0.109(1)
	b	0.108(1)
	c	0.109(1)
	d	0.109(1)
	e	0.122
C4–H6	a	0.108(1)
	b	0.107(1)
	c	0.109(1)
	d	0.109(1)
	e	0.108

multi-term Simpson's rule integration of a pseudo-Voigt function [13], while the background was fitted with a five-term cosine Fourier series. A parameter correcting for sample displacement from the focussing circle was also refined (in the present case the displacement could be due to transparency effects).

3. Results and discussion

The PPS structure problem has resulted in the publication of experimental data from different groups, which, if they do not fundamentally question the Tabor model (with the exception of Garbarczyk), differ quite significantly in the assigned cell parameters. Chung *et al.* [7] found a significant dependence of the PPS unit cell upon the thermal history of the polymer and its chemical structure (branching, molecular weight). Moreover the C–S–C angle value appears to be very critical in determining the *c*-axis parameter. The 110° value proposed by Tabor and confirmed by Lovinger *et al.* [5] on the basis of an accurate measurement of the *c* parameter, even though electron diffraction experiments, appears to be larger than the values available in the literature for PPS analogues [4, 14–16]. Attempts were thus made in the present work to check the existing models by applying the Rietveld method to PPS samples of different expected crystallinity. Unlike in other work, here the contribution due to the amorphous phase to the diffracted spectrum has been taken into account.

Using the Rietveld method it is possible to obtain simultaneously structural information (atomic position and displacement parameters) and a physical model (crystal size that determines the peak shape), which are parameters allowed to vary during the refinement until a satisfactory fit is reached between the two patterns.

The presence in all our samples of significant amounts of amorphous component is easily observed in Fig. 2 from the slowly decaying low-angle tail of the (1 1 0) peak, located at ∼19° 2θ. The four sharp peaks

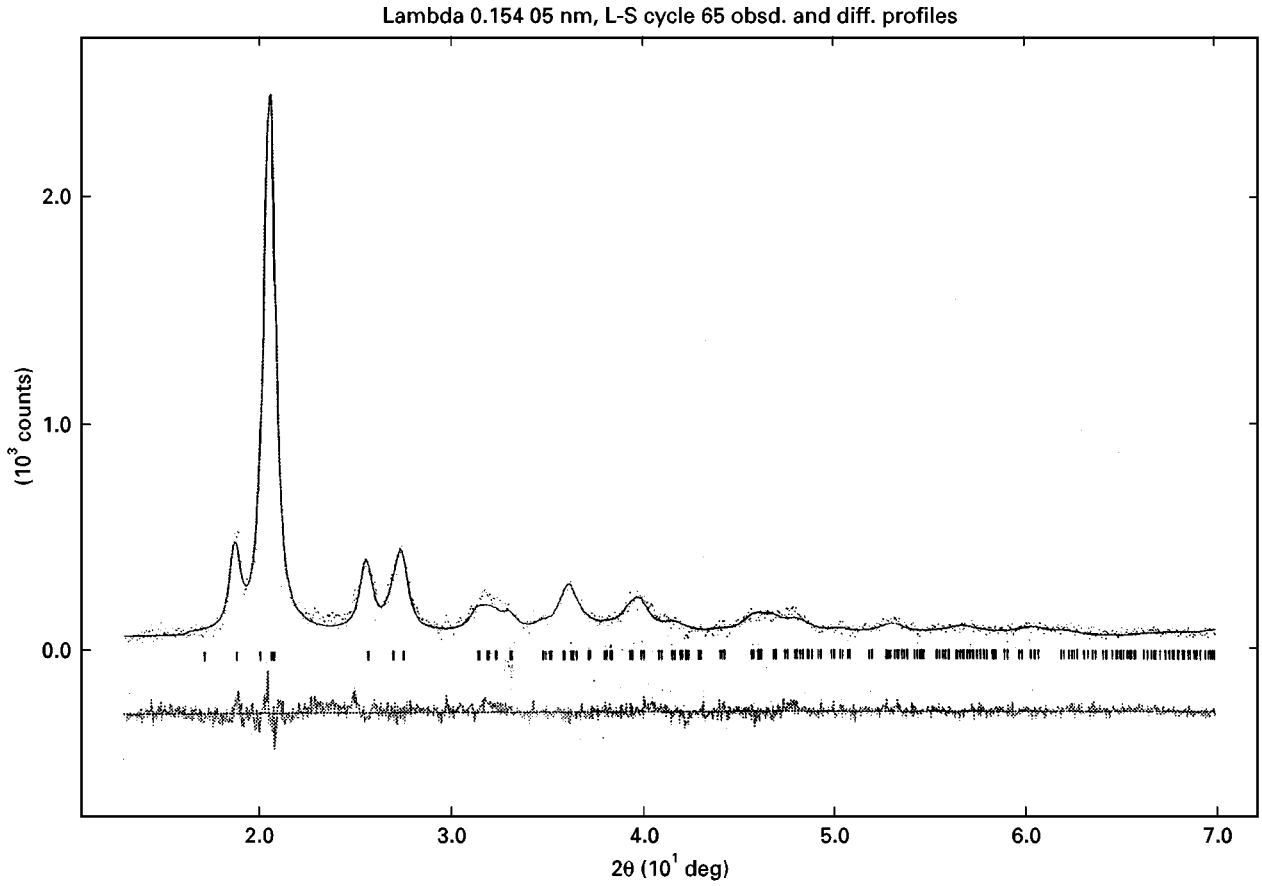

Figure 4 Example of Rietveld refinement of solution-grown sample (c-PPS). Above: (- - -) observed and (—) calculated patterns. Below: difference between experimental and calculated patterns. The vertical marks at the bottom of the observed pattern indicate the position of all the calculated $K_{\alpha 1}$ and $K_{\alpha 2}$ reflections.

TABLE V Cell parameters, unit cell volumes, density, and sample features of different PPS samples. ρ refers to the density of the crystalline phase calculated from the cell parameters

	e-PPS	c-PPS	ac130-PPS	ac210-PPS
a (nm)	0.8572(7)	0.8598(5)	0.8630(1)	0.8629(1)
b (nm)	0.5574(5)	0.5606(4)	0.5602(1)	0.5594(8)
c (nm)	1.0297(8)	1.0285(7)	1.0215(2)	1.0267(1)
Volume (nm^3)	0.4920(9)	0.4957(7)	0.4938(2)	0.4955(1)
ρ (g cm^{-3})	1.460	1.449	1.455	1.450

at $2\theta \simeq 31^\circ, 32^\circ, 42^\circ$ and 43° in the diffraction pattern of a-PPS, ac130-PPS and ac210-PPS, arise from the brass sample holder which was partly bathed by the incident X-rays.

It is well known that the presence of an amorphous component may strongly distort the peak shape, leading to peak shift. Disregarding this contribution may cause poor estimation of the position of the peaks, resulting in significant errors in the calculated cell parameters. Owing to this, the amorphous contribution, taken from the spectrum of a-PPS (even though a small crystalline fraction, less than 10%, is also present in this quenched sample) was subtracted from various diffraction patterns. The relative amount of amorphous phase was graphically estimated and subsequently adjusted in order to obtain, after the subtraction, positive intensity counts at each point on the patterns. The patterns with the amorphous component subtracted were therefore used for the Rietveld refinement (as an example, see Fig. 3).

Miscellaneous data of the refinement are reported in Table II while the structural data and bond distances are given in Tables III and IV, respectively. As examples, the experimental, calculated and difference

TABLE VI Cell parameters obtained from Rietveld refinement of (1) data with the amorphous component subtracted and (2) raw data

	e-PPS			c-PPS		
	(1)	(2)	Difference	(1)	(2)	Difference
a (nm)	0.8572(7)	0.8516(9)	0.0056	0.8598(5)	0.8559(7)	0.0039
b (nm)	0.5574(5)	0.5593(8)	− 0.0019	0.5606(4)	0.5614(6)	− 0.0008
c (nm)	1.0297(8)	1.0263(1)	0.0034	1.0285(7)	1.0279(8)	0.0006
Vol. (nm^3)	0.4920(9)	0.4888(1)	0.0033	0.4957(7)	0.4939(1)	0.0018
ρ (g cm^{-3})	1.460	1.470	1.449	1.455		

(between experimental and calculated) patterns of the solution-grown sample are shown in Fig. 4.

In our analysis the centres of gravity of the four phenylene groups were allowed to move from the special positions 0, 0, 0; 0, 0, 1/2; 1/2, 1/2, 0; and 1/2, 1/2, 1/2 that contain centres of symmetry. The displacement is relatively small and ranges between 0.006 nm and 0.024 nm. Although the standard deviations from Rietveld refinement are probably underestimated [17], the calculated C–S–C angles obtained in the present study (102°–105°) resulted in a much closer agreement with the aforementioned values for PPS analogues. Such a result did not involve a significant variation of the positional parameters which were found to be quite similar to those derived by Tabor from fibre photographs, but without assigning the large 110° value to the C–S–C angle. Table V gives the cell parameters of the various samples analysed and they are seen to differ, although not as markedly as reported by reference data for similar samples. One reason for this finding could be that Chung *et al.* [7, 8] as well as Garbarczyk [3], who reported the most significant differences in the lattice parameters compared with those of Tabor, did not take into account the amorphous contribution. In particular, Chung *et al.* [7] indicated a well-defined trend for cell parameters and annealing time and crystallization temperature. In fact, on increasing the annealing time they observed a shift of the six major diffraction peaks towards higher 2θ values. This result may be, at least in part, attributed to the decreased influence of the amorphous component, which has the maximum intensity located at $2\theta \simeq 18^\circ$ just to the left of the (1 1 0) diffraction peak. Chung *et al.* [7] however, did not indicate how the peak position was determined. This is particularly critical, especially in the case of very broad peaks, as is found with PPS (Chung *et al.* [7] estimated a full-width at half maximum (FWHM) of the order of 0.8°–0.9° 2θ for the most intense reflection).

The result of the Rietveld refinement on our e-PPS and solution-grown samples (c-PPS) seems to indicate a similar behaviour (see Table VI) with significant differences between the refinement of the raw data and the patterns with the amorphous component subtracted. In particular, these differences increase with the increased presence of amorphous component, as is indicated by the e-PPS sample ($\Delta a = 0.0056$ nm, $\Delta b = -0.0019$ nm, $\Delta c = 0.0034$ nm), characterized by the presence of a larger fraction of amorphous component than the c-PPS sample ($\Delta a = 0.0039$ nm, $\Delta b = -0.0008$ nm, $\Delta c = 0.0006$ nm). The two cold-crystallized samples ac130-PPS and ac210-PPS showed similar a and b cell parameters (difference $< \sigma$), but for the first a significantly shorter c was determined. However, because the present analysis was carried out on just a few samples, the relationship between crystallization temperature and cell parameters indicated by Chung *et al.* [7], cannot be confidently confirmed, even though in our case just the c-axis appears to be influenced by T_c.

Finally a third set of Rietveld refinements was carried out using our collected raw data, but by trying to model the amorphous contribution with a special background function that uses a straight line for the first part, and the major features of a real space correlation function for the remainder [11]. This function uses interatomic distances of the amorphous phase as refinable parameters. The fit of the diffraction pattern obtained with this kind of background function is indeed significantly improved, but the values of the derived interatomic distances for the amorphous phase were found to be not easily interpretable. In particular "ghost interatomic distances" may be introduced by Fourier truncation problems which are due to the relatively small angular range investigated with this experimental set-up. Further problems may arise from the correlation existing between the background parameters and the positional parameters of the crystalline phase.

4. Conclusion

The present study, although substantially confirming the PPS structure proposed by Tabor *et al.* in 1971, shows that the C–S–C angle value may be close to that of Garbarczyk [3] and that most often found in PPS analogues, if the centre of gravity of the four phenylene rings are allowed to move freely from the centre of symmetry of the unit cell. The resulting displacement is small and lies within 0.007–0.024 nm. The Rietveld refinements indicate that the crystallization condition (i.e. thermal history) of the samples influences the c parameter which seems to be sensitive to the crystallization temperature. The effect measured here, however, was not so remarkable, as indicated by the small variation of the atomic positional parameters of the various samples analysed (crystallized in a relatively wide range of physical conditions) and by the values of the cell parameters which do not differ from those of Tabor as markedly as previously reported by other authors [8]. This fact may be attributed to either the presence of physical differences between our samples and those studied in reference data, or the influence of the amorphous component on the calculation of the cell parameters, which may not have been taken into account by the other authors. In fact, according to our results, the amorphous component significantly distorts the peak shape, so leading to relevant peak shift.

References

1. D. G. BRADY, *J. Appl. Polym. Sci.* **20** (1976) 2541.
2. B. J. TABOR, E. P. MAGRE and J. BOON, *Eur. Polymer J.* **7** (1971) 1127.
3. J. GARBARCZYK, *Polym. Commun.* **27** (1986) 335.
4. *Idem.*, *Makromol. Chem.* **187** (1986) 2489.
5. A. UEMURA, M. TSUJI, A. KAWAGUCHI and K. I. KATAYAMA, *J. Mater. Sci.* **23** (1988) 1506.
6. A. J. LOVINGER, F. J. PADDEN and D. D. DAVIS, *Polymer* **29** (1988) 229.
7. J. S. CHUNG, J. BODZIUCH and P. CEBE, *J. Mater. Sci.* **27** (1992) 5609.
8. J. S. CHUNG and P. CEBE, *Polymer* **33** (1992) 1594.
9. L. D'ILARIO and A. PIOZZI, *J. Mater. Sci. Lett.* **8** (1989) 157.
10. L. D'ILARIO, L. LUCARINI, A. MARTINELLI and A. PIOZZI, *Eur. Polym. J.* **33(10–12)** (1997) 1809.

11. R. CAMINITI, L. D'ILARIO, A. MARTINELLI, A. PIOZZI and C. SADUN, *Macromolecules*, **30** (1997) 7970.
12. A. C. LARSON and R. B. VON DREELE, "GSAS General Structure Analysis System", LAUR 86-748, Los Alamos National Laboratory, Copyright. 1985–1994 (The Regents of the University of California, 1985).
13. C. J. HOWARD, *J. Appl. Crystallogr* **15** (1982) 615.
14. B. ROZSONDAI, G. SCHULTZ and I. HARGITTAI, *J. Molec Struct*. **70** (1981) 309.
15. M. SACERDOTI, V. BERTOLASI and G. GILLI, *Cryst. Struct. Commun.* **5** (1976) 477.
16. V. CODY and F. P. A. LEHMANN, *ibid.* **11** (1982) 1671.
17. J. F. BERAR and P. LELANN, *J. Appl. Crystallogr.* **24** (1991) 1.

Received 3 November 1997
and accepted 22 April 1998